Supplemental material for: Fundamental limits on the rate of bacterial cell division

Nathan M. Belliveau[1,*], **Griffin Chure**[2,3,*], **Christina L. Hueschen**[4], **Hernan G. Garcia**[5], **Jané Kondev**[6], **Daniel S. Fisher**[7], **Julie Theriot**[1,8], **Rob Phillips**[1,9,†]

***For correspondence:**

[*]These authors contributed equally to this work

[1]Department of Biology, University of Washington, Seattle, WA, USA; [2]Division of Biology and Biological Engineering, California Institute of Technology, Pasadena, CA, USA; [3]Department of Applied Physics, California Institute of Technology, Pasadena, CA, USA; [4]Department of Chemical Engineering, Stanford University, Stanford, CA, USA; [5]Department of Molecular Cell Biology and Department of Physics, University of California Berkeley, Berkeley, CA, USA; [6]Department of Physics, Brandeis University, Waltham, MA, USA; [7]Department of Applied Physics, Stanford University, Stanford, CA, USA; [8]Allen Institute for Cell Science, Seattle, WA, USA; [9]Department of Physics, California Institute of Technology, Pasadena, CA, USA; [†]Address correspondence to phillips@pboc.caltech.edu; [*]Contributed equally

Summary of Proteome Datasets.

[NB: in progress. I think one useful figure for me to make is a schematic showing how absolute copy numnbers were determined in each paper we considered.]

Summary of final compiled data set.

[NB: in progress]

Adjustments to Schmidt *et al.* dataset

While the dataset from Schmidt *et al.* remains a heroic effort that our lab continues to return to as a resource, there were steps taken in their calculation of protein copy number that we felt needed some further consideration. In particular, the authors made an assumption of constant cellular protein concentration across all growth conditions and used measurements of cell volume that appear inconsistent with an expected exponential scaling of cell size with growth rate that is well-documented in *E. coli* (***Schaechter et al.*** (***1958***); ***Taheri-Araghi et al.*** (***2015***); ***Si et al.*** (***2017***)).

We begin by looking at their cell volume measurements, which are shown in blue in Figure 1. As a compairon, we also plot cell sizes reported in three other recent papers: measurements from Taheri-Araghi *et al.* and Si *et al.* come from the lab of Suckjoon Jun, while those from Basan *et al.* come from the lab of Terence Hwa. Each set of measurements used microscopy and cell segmentation to determine the length and width, and then calculated cell size by treating the cell is a cylinder with two hemispherical ends. While there is a large discrepancy in cell size between the two research groups, Basan *et al.* found that this came specifically from uncertainty in determining the cell width, which is prone to inaccuracy given the small cell size and optical resolution limits (further described in their supplemental text). Perhaps the more concerning point is that while each of these alternative measurements show an exponential increase in cell size at faster growth rates, the measurements used by Schmidt *et al.* appear to plateau. This resulted in an analogous trend in their final reported total cellular protein per cell as shown in Figure 2 (purple data points), and is in disagreement with other measurements of total protein at these growth rates (***Basan et al.*** (***2015***)).

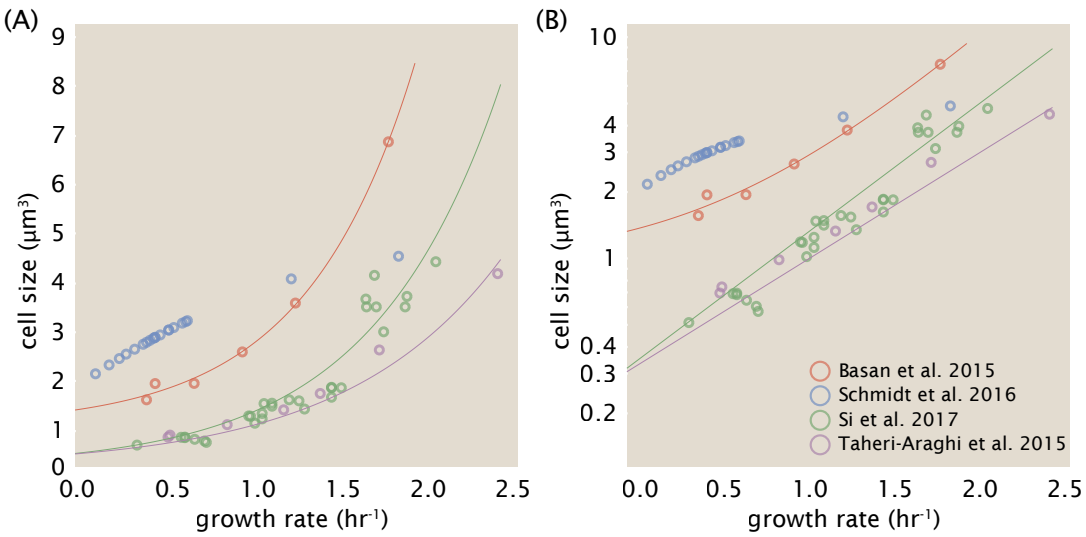

Figure 1. Measurements of cell size as a function of growth rate. (A) Plot of the reported cell sizes from several recent papers. The data in blue come from Volkmer and Heinemann, 2011 (***Volkmer and Heinemann*** (***2011***)) and were used in the work of Schmidt *et al.*. Data from the lab of Terence Hwa are shown in red (***Basan et al.*** (***2015***)), while the two data sets shown in green and purple come from the lab of Suckjoon Jun (***Taheri-Araghi et al.*** (***2015***); ***Si et al.*** (***2017***)). (B) Same as in (A) but with the data plotted on a logarithmic y-axis to highlight the exponential scaling that is expected for *E. coli*.

Since it is not obvious how measurements of cell size might have influenced their reported protein abundances, we will go through this calculation in the next section. We will also show how these can adjusted to better reflect the alternative measurements of cell size shown in Figure 1. Finally, we consider several strategies to adjust the reported copy numbers, with the result summarized in Figure 2. For most growth conditions, we find that total protein expectations are not expected to change dramatically. However, for the fastest growth conditions, with glycerol + supplemented amino acids, and LB media, there is quite a bit of variability among are different estimates.

Effect of cell volume on reported absolute protein abundances in the work of Schmidt *et al.* .

The authors calculated proteome-wide protein abundance by first determining absolute abundances of 41 pre-selected proteins, which relied on adding synthetic heavy reference peptides into their protein samples at known abundance (with proteins selected to cover the range of expected copy numbers). This absolute quantitation was performed in replicate for each growth condition. Separately, the authors also performed a more conventional mass spectrometry measurement for samples from each growth condition, which attempted to maximize the number of quantified proteins but only provided relative abundances based on peptide intensities. Finally, using their 41 proteins with absolute abundances already determined, they then created calibration curves with which to relate their relative intensity to absolute protein abundance for each growth condition. This allowed them to estimate absolute protein abundance for all proteins detected in their proteome-wide data set. Combined with their flow cytometry cell counts, they were then able to determine absolute abundance of each protein detected on a per cell basis.

While this approach provided absolute abundances, another necessary step needed to arrive at total cellular protein is to account for any protein loss during their various protein extraction steps. Here the authors attempted to determine total protein separately using a BCA protein assay. In personal communications, it was noted that determining reasonable total protein abundances by BCA across their array of growth conditions was particularly troublesome. Instead, they noted

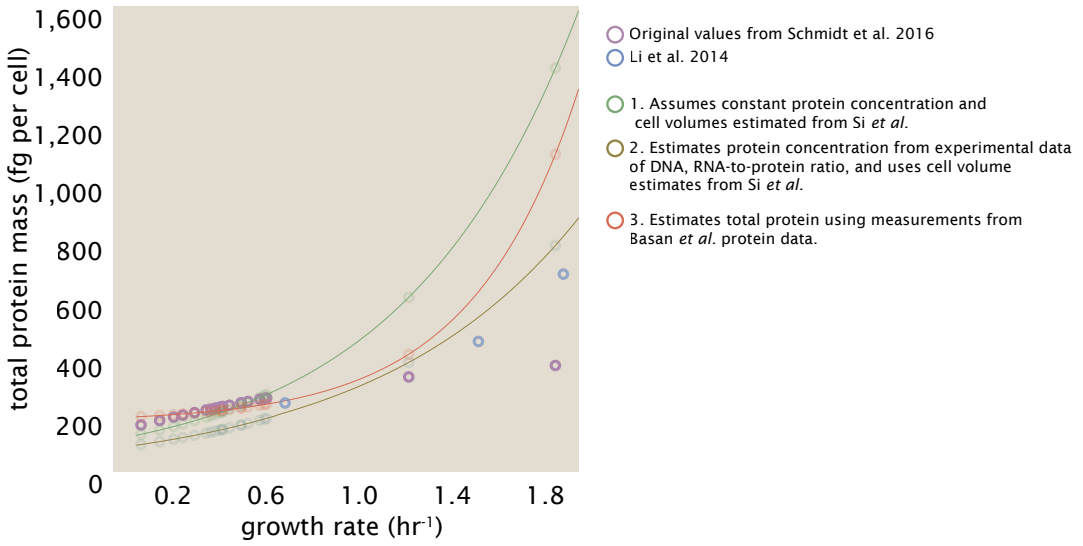

Figure 2. Alternative estimates of total cellular protein for the growth conditions considered in Schmidt *et al.* The original protein mass from Schmidt *et al.* and Li *et al.* are shown in purple and blue, respectively. *Green*: Rescaling of total protein mass assuming a growth rate independent protein concentration and cell volumes estimated from Si *et al.* 2017. *Gold*: Rescaling of total protein mass using estimates of growth rate-dependent protein concentrations and cell volumes estimated from Si *et al.* 2017. *Red*: Rescaling of total protein mass using the experimental measurements from Basan *et al.* 2015.

confidence in their total protein measurements for cells grown in M9 minimal media + glucose and used this as a reference point with which to estimate the total protein for all other growth conditions.

For cells grown in M9 minimal media + glucose an average total mass of M_P = 240 fg per cell was measured. Using their reported cell volume, reported as V_{orig} = 2.84 fl, a cellular protein concentration of $[M_P]_{orig} = M_P/V_{orig}$ = 85 fg/fl. Now, taking the assumption that cellular protein concentration is relatively independent of growth rate, they could then estimate the total protein mass for all other growth conditions from,

$$M_{P\_i} = [M_P]_{orig} \cdot V_i \quad (1)$$

where M_{P_i} represents the total protein mass per cell and V_i is the cell volume for each growth condition i as measured in Volkmer and Heinemann, 2011. Here the thinking is that the values of M_{P_i} reflects the total cellular protein for growth condition i, where any discrepancy from their absolute protein abundance is assumed to be due to protein loss during sample preparation. The protein abundances from their absolute abundance measurements noted above were therefore scaled to their estimates and are shown in Figure 2 (purple data points).

If we instead consider the cell volumes predicted in the work of Si *et al.*, we again need to take growth in M9 minimal media + glucose as a reference with known total mass, but we can follow a similar approach to estimate total protein mass for all other growth conditions. Letting V_{Si_glu} = 0.6 fl be the predicted cell volume, the cellular protein concentration becomes $[M_P]_{Si} = M_P/V_{Si\_glu}$ = 400 fg/fl. The new total protein mass per cell can then be calculated from,

$$M'_{P\_i} = [M_P]_{Si} \cdot V_{Si\_i} \quad (2)$$

where M'_{P_i} is the new protein mass prediction, and V_{Si_i} refers to the new volume prediction for each condition i, These are shown as [] dots in Figure 2.

Reconsidering assumption that protein concentration is constant.

We next relax the assumption that cellular protein concentration is constant and instead, attempt to estimate it using experimental data. Here we first note that for across almost the entire range of growth rates considered here, protein, DNA, and RNA accounted for at least 90 % of the dry mass in measurements from the lab of Terence Hwa (***Basan et al.*** (***2015***)). They also found that the total dry mass concentration was roughly constant across growth conditions. Under such a scenario, we can calculate the total dry mass concentration for protein, DNA, and RNA, which is given by 1.1 g/ml x 30 % x 90 % or about $[M_P]$ = 300 fg per fl. Using the cell volume predictions from Si *et al.*, we can then calculate the associated mass per cell.

However, even if dry mass concentration is relatively constant across growth conditions, it is not a given that protein concentration should also be constant. In particular, we know that rRNA increases substantially at faster growth rates (***Dai et al.*** (***2016***)). This is a well-documented result that arises from an increase in the fraction of ribosomes at faster growth rates (***Scott et al.*** (***2010***)). To proceed we will use therefore rely on experimental measurements of total DNA content per cell that also come from Basan *et al.*, and RNA to protein ratios that were measured in Dai *et al.* (and cover the entire range of growth conditions considered here). These are reproduced in Figure 3(A) and (B), respectively.

Assuming that the protein, DNA, and RNA account for 90 % of the total dry mass, the protein mass can then determined by first subtracting the experimentally measured DNA mass, and then using the experimental estimate of the RNA to protein ratio. The total protein per cell is will be related to the summed RNA and protein mass by,

$$M_P = \frac{[M_P + M_{RNA}]}{1 + (RP_{ratio})}. \tag{3}$$

(RP_{ratio} refers to the RNA to protein ratio as measured by Dai *et al.*. In Figure 3(C) we plot the estimated cellular concentrations for protein, DNA, and RNA from these calculations, and in Figure 3(D) we plot their total expected mass per cell.

Estimating cellular protein concentration as a function of growth rate.

One of the challenges in our estimates in the preceding sections is the need to estimate protein concentration and cell volumes. These are inherently difficult to to accurately due to the small size of *E. coli*. Indeed, for all the additional measurements of cell volume included in Figure 1, no measurements were performed for cells growing at rates below 0.5 hr^{-1}. It therefore remains to be determined whether our extrapolated cell volume estimates are appropriate, with the possibility that the logarithmic scaling of cell size might break down for slower growth.

In our last approach we therefore attempt to estimate total protein using experimental data that required no estimates of concentration or cell volume. Specifically, in the work of Basan *et al*, the authors measured total protein per cell for a broad range of growth rates (reproduced in Figure 4). These were determined by first measuring bulk protein from cell lysate, measured by the colorimetric Biuret method (***You et al.*** (***2013***)), and then abundance per cell was calculated from cell counts from either plating cells or a Coulter counter. While it is unclear why Schmidt *et al.* was unable to take a similar approach, the results from Basan *et al* appear more consistent with our expectation that cell mass will increase exponentially with faster growth rates. In addition, although they do not consider growth rates below about 0.5 hr^{-1}, it is interesting to note that the protein mass per cell appears to plateau to a minimum value at slow growth. In contrast, our estimates using cell volume so far have predicted that total protein mass should continue to decrease slightly for slower growing cells. By fitting this data to an exponential function dependent on growth rate, we could then estimate the total protein per cell for each growth condition considered by Schmidt *et al.*. These are plotted in red in Figure 2.

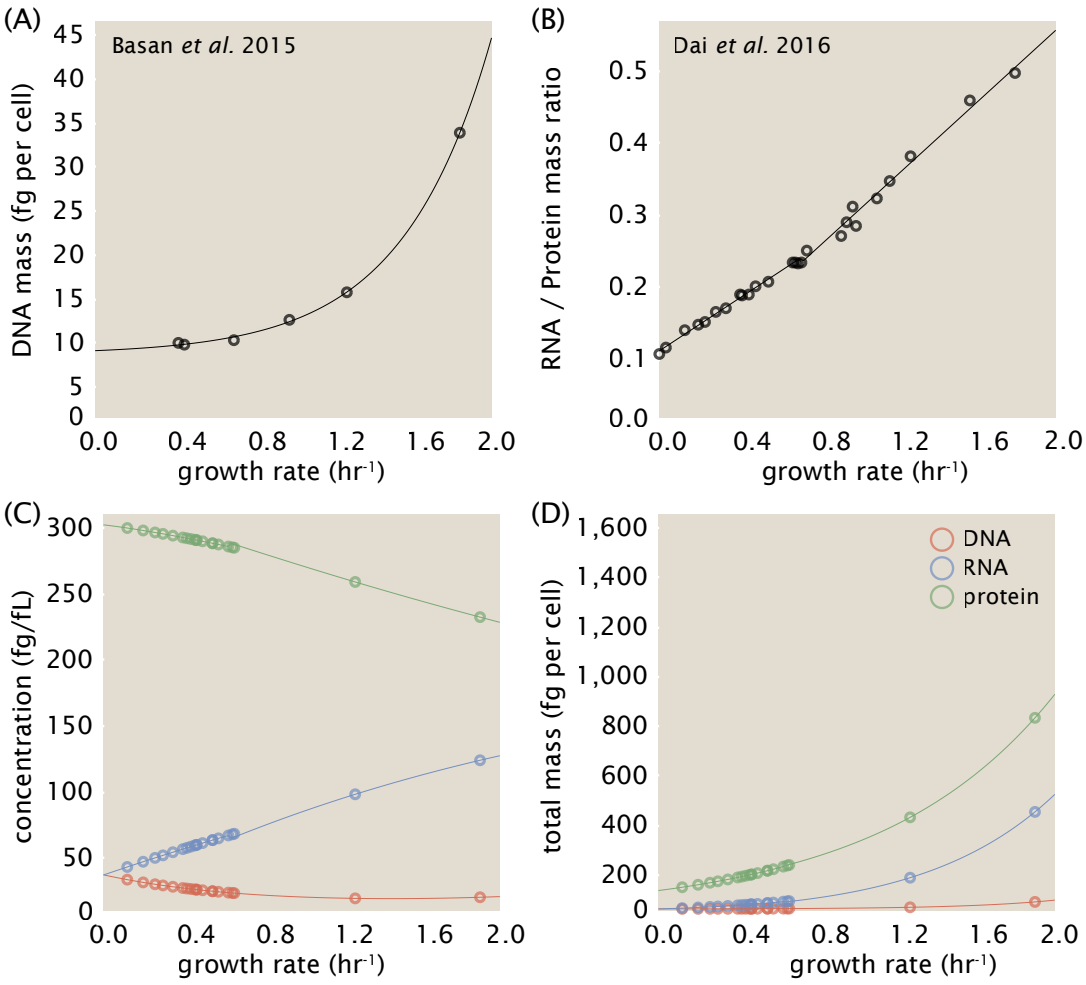

Figure 3. Empirical estimate of cellular protein, DNA, and RNA as a function of growth rate. (A) Measured DNA mass per cell as a function of growth rate, reproduced from Basan *et al.* 2015. The data was fit to an exponential curve (DNA mass in fg per cell is given by 0.42 $e^{2.23 \cdot \lambda}$ + 7.2 fg per cell, where λ is the growth rate in hr^{-1}). (B) RNA to protein measurements as a function fo growth rate. The data was for to two lines: for growth rates below 0.7 hr^{-1}, the RNA/protein ratio is $0.18 \cdot \lambda + 0.093$, while for growth rates faster than 0.7 hr^{-1} the RNA/protein ratio is given by $0.25 \cdot \lambda + 0.035$. For (A) and (B) cells are grown under varying levels of nutrient limitation, with cells grown in minimal media with different carbon sources for the slowest growth conditions, and rich-defined media for fast growth rates. (C) Predictions of cellular protein, DNA, and RNA concentration. (D) Total cellular mass predicted for protein, DNA, and RNA using the cell size predictions from Si *et al.*

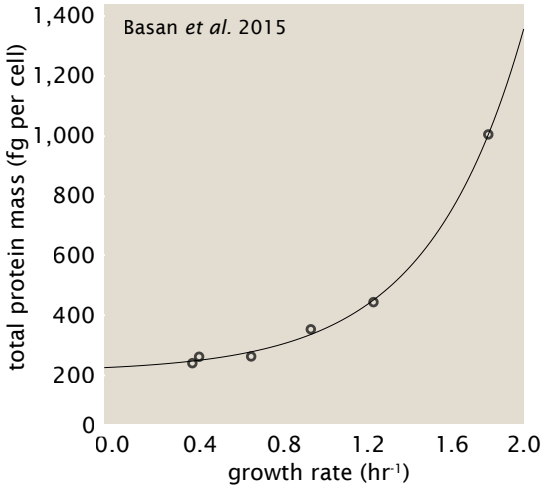

Figure 4. Total cellular protein reported in Basan *et al.* 2015. Measured protein mass as a function of growth rate as reproduced from Basan *et al.* 2015, with cells grown under different levels of nutrient limitation. The data was fit to an exponential curve where protein mass in fg per cell is given by 14.65 $e^{2.180 \cdot \lambda}$ + 172 fg per cell, where λ is the growth rate in hr^{-1}).

Estimation of cell size and surface area.

In Figure 1 we looked at a number of recent cell size measurements and potential issues with the values used by Schmidt *et al.*. Since most of our data sets lacked any cell size measurements, we chose instead to use a common set of size measurements for any analysis that required calculation of cell size or surface area. Here we compile the cell size measurements from the recent works of Si *et al.* 2017, 2019, which covers almost the entire range of growth rates considered across the proteomic data (shown in Figure 5). In each dataset, the authors made measurements on strains MG1655 and NCM3722, which each appear to show a logarithmic scaling with growth rate.

Since each of our proteomic datasets use either K-12 MG1655 or its derivative BW25113 (from the lab of Barry L. Wanner; the parent strain of the Keio collection (***Datsenko and Wanner, 2000***; ***Baba et al., 2006***)), we only considered the MG1655 size data. The length and width measurements were well described by 0.5 $e^{1.09 \cdot \lambda}$ + 1.76 μ m, and 0.64 $e^{0.24 \cdot \lambda}$ μ m, respectively. In order to estimate cell size we take the cell as a cylinders with two hemispherical ends (***Si et al., 2017***; ***Basan et al., 2015***). Specifically, cell size (or volume) is estimated from,

$$V = \pi \cdot r^2 \cdot (l - 2r/3), \tag{4}$$

where r is half the cell width. A best fit to the data described by 0.533 $e^{1.037 \cdot \lambda}$ μ m^3. Calculation of the cell surface area is given by,

$$S = \eta \cdot \pi (\frac{\eta \cdot \pi}{4} - \frac{\pi}{12})^{-2/3} V^{2/3}, \tag{5}$$

where η is the aspect ratio ($\eta = l/w$) (***Ojkic et al., 2019***).

Changes to translation under nutrient-limitation.

In the work of Dai et al. the authors demonstrated that a number of important changes take place with respect to translation for cells growing under extents of nutrient limitation. Specifically, as the growth rate decreases, the translation elongation rate decreases from a maximum of about 17 aa/s to 8 aa/s in stationary phase. Addition of sub-lethal doses of chloramphenicol, which bind the []S ribosomal subunit and prevent translation, caused an increase in elongation rate albeit at the consequence of slower growth. Lastly, for growth rates below about 0.7 hr^{-1}, the measured growth rates were inconsistent with that required for mass balance of a doubling cell

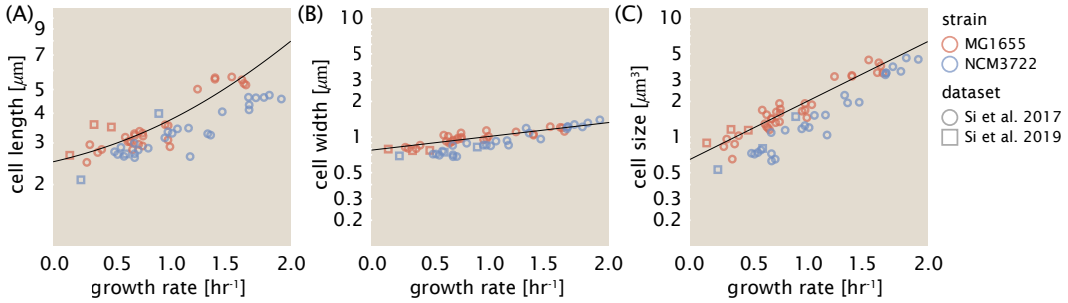

Figure 5. Summary of size measurements from Si *et al.* 2017, 2019. Cell lengths and widths were measured from cell contours obtained from phase contrast images, and refer to the long and short axis respectively. (A) Cell lengths and (B) cell widths show the mean measurements reported (they report 140-300 images and 5,000-30,000 for each set of samples; which likely means about 1,000-5,000 measurements per mean value reported here since they considered about 6 conditions at a time). Fits were made to the MG1655 strain data; length: 0.5 $e^{1.09\cdot\lambda}$ + 1.76 μ m, width: 0.64 $e^{0.24\cdot\lambda}$ μ m. (C) Cell size, V, was calculated as cylinders with two hemispherical ends (Equation 4). The MG1655 strain data gave a best fit of 0.533 $e^{1.037\cdot\lambda}$ μ m^3.

given the independently measured elongation rates and ribosomal abundance. This suggests that the cell is also regulating, either actively or passively, the fraction of translating ribosomes in this nutrient-limited regime.

In that work they propose that there may be a bottleneck in translation that arises due to lower availability of ternary complex (TC) that must bind the ribosome in order for translation to proceed. This complex consists of aminoacyl-tRNA, elongation factor Tu and guanosine triphosphate. To account for this bottleneck, they divide the elongation rate into two coarse-grained timescales: A) binding of the ternary complex to the ribosome, which will depend inversely on the effective TC concentration $[TC_{eff}]$, and B) other enzymatic processes that will not depend on TC concentration. Letting these two timescales be $1/(k_{on}\cdot[TC_{eff}])$ and $1/r_t$, the new elongation rate is given by,

$$\frac{1}{r_t} = \frac{1}{k_{on}\cdot[TC_{eff}]} + \frac{1}{r_t^{max}} \tag{6}$$

where r_t/k_{on} is the binding constant of the TC with the ribosome. Further taking $[TC_{eff}]$ to be proportional to the RNA/protein ratio,

$$[TC_{eff}] = C\cdot(R_m/P_m), \tag{7}$$

they find that r_t = 22 aa/s, k_{on} = 6.4 $\mu M^{-1}s^{-1}$, and C = 31 μM.

The above model follows a hypothesis that there is a bottleneck in the availability of ternary complex, referring to the complex of aminoacyl-tRNA, elongation factor Tu and guanosine triphosphate (GTP) that is needed for translation. However, if cells are indeed reducing their fraction of actively translating ribosomes as inferred in the work of Dai *et al.*, it is difficult to rationalize the possibility that it is a protein like Tu that is limiting. Under such a situation, a simple solution would be for the cell to synthesize more Tu proteins at the expense of making fewer of the unused ribosomes. In contrast, at least in the limit of poorer nutrient conditions, the possibility of limitations on more basic building blocks like amino acids and GTP seem more reasonable. We next therefore consider the case where the synthesis of amino acids, and therefore the cellular concentration of amino acids $[aa]_{eff}$ and charged-tRNA is limiting.

Here we follow a similar approach to that employed by Dai *et al.*, which is to divide the elongation rate into two coarse-grained timescales. Here we assume that the elongation rate depends on A) binding of a ternary complex, which we instead propose depends on a rate-limiting concentration of $[aa]_{eff}$ and, 2) other enzymatic processes that will not depend on $[aa]_{eff}$. The effective elongation

rate is given by the inverse timescales associated with each step,

$$\frac{1}{r_t} = \frac{1}{k_{on} \cdot [aa]_{eff}} + \frac{1}{r_t^{max}}. \tag{8}$$

where r_t is the measured elongation rate, r_t^{max} is the maximum elongation rate, and r_t^{max}/k_{on} is the binding constant K_d of the ternary complex with the ribosome. Alternatively, we can re-write this in terms of the binding constant,

$$r_t = r_t^{max} \cdot \frac{1}{1 + K_d/[aa]_{eff}}. \tag{9}$$

[note value of $[aa]_{eff}$ $from Bennett] If we consider only consumption of amino acids by ribosomes, during steady state grou$ will be depend on the amino acid synthesis rate r_{aa}, consumption rate by ribosomes, $R \cdot r_t$, and the cell volume V,

$$\frac{d[aa]_{eff}}{dt} = r_{aa} - r_t \cdot R \cdot f_a \cdot [aa]_{eff}. \tag{10}$$

Here, the factor $R \cdot f_a$ reflects the number of 'ribosome equivalents' that are actively translating and allows us to account for ribosomes not engaged in translation. This may be either due to active regulation by the cell, or the result of improperly assembled ribosomes or abortive ribosomal products. Under steady-state growth we can set the left-hand side to zero and solve for $[aa]_{eff}$,

$$[aa]_{eff} = \frac{r_{aa}}{r_t \cdot R \cdot f_a}. \tag{11}$$

Plugging this in, we are left with,

$$r_t = \frac{r_{t^{max}}}{1 + K_d \cdot \frac{r_t \cdot R \cdot f_a}{r_{aa}}}. \tag{12}$$

It is worth noting that here we see that the elongation rate should indeed depend on the ribosomal abundance, at least in how it is related to number of ribosomes R ($R \approx \Phi_R \cdot N_{aa}/L_R \propto (R_m/P_m) \cdot N_{aa}/L_R$). However, in contrast to the model presented by Dai *et al.*, an increase in R (or R_m/P_m) predicts a decrease in r_t since this will lead to a lower $[aa]_{eff}$ (see Equation 9).

We also note another important point given the experimental observation that the elongation rate does not drop to zero aa/s at very slow growth. At some point, when nutrient conditions are sufficiently poor, ribosomes will be in excess of the rate with which the cell can synthesize them. In this regime ribosomes would deplete their amino acid supply and be unable to maintain steady-state growth. Rather, a bacterium will need to decrease its pool of actively translating ribosomes in order to maintain a constant growth rate. This at least provides us with some rationalization for why a cell would apparently regulate its fraction of ribosomes actively engaged in translation in poor nutrient conditions.

In Equation 12 we see that the elongation rate r_t will itself depend on r_t. This is because r_t, along with the number of ribosomes R, dictate how quickly amino acids are consumed. In order to solve for r_t explicitly we note that this is a quadratic equation of r_t and we can solved by finding its roots. These are given by,

$$r_t = \frac{+/- \sqrt{4 \cdot K_d \cdot R \cdot f_a \cdot r_{t^{max}}/r_{aa} + 1} - 1}{2 \cdot K_d \cdot R \cdot f_a / r_{aa}}, \tag{13}$$

where we can ignore the root containing a negative square root term since this results in a negative elongation rate.

In the main text we suggest that the increase in R observed at faster growth rates is in part a consequence of how the cell biases ribosomal gene dosage, and increases it's overall biomass. Here we also expect r_{aa} to increase in more nutrient rich media, since it reflects the synthesis rate of amino acids (or supply rate, when their imported from the media). Conversely, for a specific

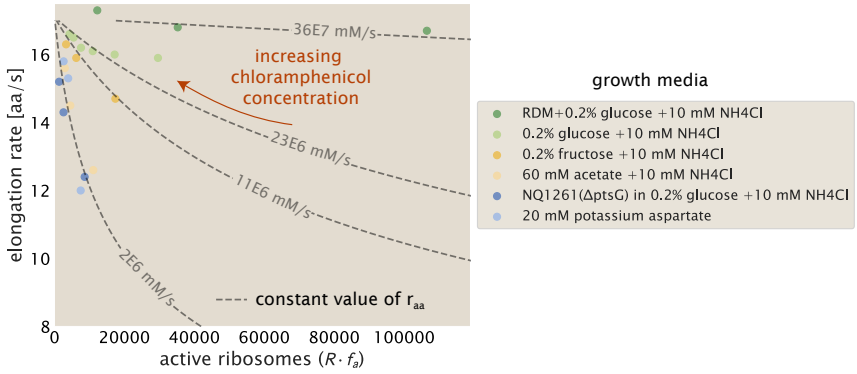

Figure 6. .

growth condition we expect r_{aa} will remain relatively constant if the number of ribosomes were perturbed. As a test of this hypothesis, we consider additional data from Dai *et al.* where sub-lethal doses of chloramphenicol were added to the media. In these experiments, they measured the RNA-to-protein ratio R_m/P_m, elongation rate r_t, and from their measurements of growth rate inferred f_a from the requirement of mass balance (i.e. how much time would have been needed to double to cell contents given their measured elongation rate). In order to estimate the number of active ribosomes here, and in Figure 7 of the main text, we have calculated the ribosomal mass fraction using their reported RNA-to-protein ratios ($\Phi_R \approx 2.1 \cdot R_m/P_m$ ***Dai et al.*** (***2016***)) and then estimated the number of active ribosomes from $R \cdot f_a \approx (\Phi_R \cdot N_{aa}/L_R) \cdot f_a$.

Figure 6 shows this data, along with dashed lines of constant $r_a a$ based on Equation 13. Consistent with our hypothesis, we find that the fraction of active ribosomes and elongation rate vary along line of roughly constant $r_a a$ for each growth condition. This is even though cells were found to increase their RNA-to-protein ratio with increasing concentrations of chloramphenicol. One point of caution here is that since the ribosomal fraction ($\propto R_m/P_m ratio) was found to vary with chloramphenicol concentratio$ Further experimental work would be needed to more carefully test our predictions under perturbations like that performed with chloramphenicol.

As a final point, it is now possible to consider how the translation-limited growth rate might vary as the parameters R, f_a, and r_t by using Equation 1 from the main text. This is re-written here for convienence,

$$\lambda_{\text{translation-limited}} \approx \frac{ln(2) \cdot r_t}{L_R} \Phi_R. \tag{14}$$

In the slow growth regime (0.5 hr^{-1} or slower), Φ_R does not vary as dramatically as at fast growth and in Figure 7(E) of the main text we created a heatmap of growth rate across this parameter space by assuming a constant value Φ_R=0.13.

References

Baba, T., Ara, T., Hasegawa, M., Takai, Y., Okumura, Y., Baba, M., Datsenko, K. A., Tomita, M., Wanner, B. L., and Mori, H. (2006). Construction of Escherichia coliK-12 in-frame, single-gene knockout mutants: the Keio collection. *Molecular Systems Biology*, 2(1):2460.

Basan, M., Zhu, M., Dai, X., Warren, M., Sévin, D., Wang, Y.-P., and Hwa, T. (2015). Inflating bacterial cells by increased protein synthesis. *Molecular Systems Biology*, 11(10):836.

Dai, X., Zhu, M., Warren, M., Balakrishnan, R., Patsalo, V., Okano, H., Williamson, J. R., Fredrick, K., Wang, Y.-P., and Hwa, T. (2016). Reduction of translating ribosomes enables Escherichia coli to maintain elongation rates during slow growth. *Nature Microbiology*, 2(2):16231.

Datsenko, K. A. and Wanner, B. L. (2000). One-step inactivation of chromosomal genes in Escherichia coli K-12 using PCR products. *Proceedings of the National Academy of Sciences*, 97(12):6640–6645.

253 Ojkic, N., Serbanescu, D., and Banerjee, S. (2019). Surface-to-volume scaling and aspect ratio preservation in
254 rod-shaped bacteria. *eLife*, 8:642.

255 Schaechter, M., MaalØe, O., and Kjeldgaard, N. O. (1958). Dependency on Medium and Temperature of Cell Size
256 and Chemical Composition during Balanced Growth of Salmonella typhimurium. *Microbiology*, 19(3):592–606.

257 Scott, M., Gunderson, C. W., Mateescu, E. M., Zhang, Z., and Hwa, T. (2010). Interdependence of cell growth and
258 gene expression: origins and consequences. *Science*, 330(6007):1099–1102.

259 Si, F., Li, D., Cox, S. E., Sauls, J. T., Azizi, O., Sou, C., Schwartz, A. B., Erickstad, M. J., Jun, Y., Li, X., and Jun, S. (2017).
260 Invariance of Initiation Mass and Predictability of Cell Size in Escherichia coli. *Current Biology*, 27(9):1278–1287.

261 Taheri-Araghi, S., Bradde, S., Sauls, J. T., Hill, N. S., Levin, P. A., Paulsson, J., Vergassola, M., and Jun, S. (2015).
262 Cell-size control and homeostasis in bacteria. *Current Biology*, 25(3):385–391.

263 Volkmer, B. and Heinemann, M. (2011). Condition-Dependent Cell Volume and Concentration of Escherichia coli
264 to Facilitate Data Conversion for Systems Biology Modeling. *PLOS ONE*, 6(7):e23126.

265 You, C., Okano, H., Hui, S., Zhang, Z., Kim, M., Gunderson, C. W., Wang, Y.-P., Lenz, P., Yan, D., and Hwa, T. (2013).
266 Coordination of bacterial proteome with metabolism by cyclic AMP signalling. *Nature*, 500(7462):301–306.